ELSEVIER

Marine Geology 190 (2002) 591–608

MARINE GEOLOGY
INTERNATIONAL JOURNAL OF MARINE GEOLOGY, GEOCHEMISTRY AND GEOPHYSICS

www.elsevier.com/locate/margeo

Morphodynamics of intertidal bar morphology on a macrotidal beach under low-energy wave conditions, North Lincolnshire, England

Aart Kroon [a,*], Gerhard Masselink [b]

[a] *Institute for Marine and Atmospheric Research Utrecht, Department of Physical Geography, Utrecht University, P.O. Box 80115, 3508 TC Utrecht, The Netherlands*

[b] *Department of Geography, University of Loughborough, Loughborough, Leicestershire, LE11 3TU, UK*

Received 27 December 2001; accepted 12 July 2002

Abstract

The morphological changes of multiple intertidal bars (ridges) on a macrotidal beach were examined under low-energy wave conditions during a spring-to-spring tidal cycle. The morphological response was coupled to the tidal water level variations and related residence times for swash processes and surf (breaking waves and bores) over the cross-shore profile. Spring tides induced a large spatial variation in water lines and small residence times for distinct processes. Neap tides narrowed the intertidal area and increased the time for certain processes to work on the sediment at one location. The observed morphological changes could be coupled to the stagnation of processes at a certain bar crest position. The action of surf (breaking waves and bores) played the major role in the onshore migration of the intertidal bars and the simultaneous erosion of the seaward flank. Swash action, responsible for the generation and migration of intertidal bars in microtidal settings, was not the dominant process in causing the observed morphological changes. Intertidal ridges on macrotidal beaches cannot be considered swash bars as suggested by most previous investigations into these morphological features.

Keywords: beach; intertidal bars; ridge; runnel; macrotidal; swash; bores

1. Introduction

Intertidal bar morphology is common on many tidal beaches. The morphodynamics of such intertidal bar systems are primarily controlled by the tidal range and the incident wave energy level and variability. Two types of intertidal bar systems can loosely be identified. On beaches subjected to small tidal ranges (< 3 m) there is generally only space enough for a single intertidal bar/trough system. Such bars may originally have developed near the low-water line and migrated onshore towards the upper beach (berm) following low-energy wave conditions (Hayes and Boothroyd, 1969; Davis et al., 1972; Owens and Frobel, 1977; Wijnberg and Kroon, in press). Their presence and migration are therefore indicative of onshore sediment transport and their morphology characterised by distinct landward slip faces testi-

* Corresponding author. Tel: +31-30-2533864; fax: +31-30-2531145.
E-mail address: a.kroon@geog.uu.nl (A. Kroon).

0025-3227/02/$ – see front matter
PII: S0025-3227(02)00475-9

fies this. Such intertidal bars finally merge or weld with the berm, or flatten as a result of macro-scale beach profile adjustment following storm erosion. On those beaches subjected to large tidal ranges (>3 m), the intertidal zone is wide enough to accommodate a number of intertidal bar/trough systems. Here, however, the bars appear not to be related to macro-scale beach profile adjustment (Mulrennan, 1992), but are thought to be associated with local adjustments of the beach gradient (King and Williams, 1949; King, 1972). Such intertidal bars are relatively stationary features and generally do not have a pronounced asymmetric cross-shore profile with a slip face (Mulrennan, 1992; Sipka and Anthony, 1999).

The present study is concerned with the morphodynamics of multiple intertidal bar systems. The type of morphology under consideration is generally known as 'ridge and runnel' morphology, a term introduced by King and Williams (1949) to describe the morphological highs and intervening lows found in the intertidal zones of some fetch-limited, macrotidal beaches in England and France. According to King and Williams (1949), the ridges are intertidal swash bars that have survived tidal immersion. King (1972, p. 343) further suggested that 'ridges and runnels are the result of an attempt by the waves to produce an equilibrium swash zone gradient, suitable to their dimensions, on a beach the overall gradient of which is flatter than the equilibrium gradient'. The notion that the ridges are intertidal swash bars has become more or less entrenched in the coastal literature (Orford and Wright, 1978). It seems prudent, however, to briefly review on what basis it has been deduced that the ridges are formed by swash processes. In laboratory experiments reported by King and Williams (1949) it was shown that a bar formed by breaking waves ('breaker bar') was flattened, if not destroyed by a falling water level. A ridge formed by high-tide swash processes ('swash bar'), on the other hand, was left undisturbed by a falling water level. On the basis of these results, King and Williams (1949, p. 84) felt justified to conclude 'a tentative correlation (...) of swash bars with the ridges found on some tidal beaches'. King and Williams (1949) also noted that the upper part of the seaward slope of ridges on natural beaches is generally smooth and this provided their second reason for presuming that the ridges are formed by the same agencies as swash bars. King (1972, p. 344) argued that 'where waves are adjusting the gradient of the swash slope to suit their dimensions the process will continue most effectively where the waves are at specific levels for the longest period on a tidal beach'. Carrying this argument through, King (1972) postulated that these levels will be the position of the mean low spring and neap tides and found this hypothesis confirmed by long-term field observations conducted on Blackpool beach.

When the cumulative evidence put forward by King and Williams (1949) and King (1972) to support a swash origin of the ridges is considered in a fresh light it does not seem to hold up very well. Firstly, the laboratory experiments were rather inconclusive. For example, no attempt was made to form swash bars in the intertidal zone, so the effect of falling water levels on intertidal swash bars was not investigated. The fact that the seaward slopes of the ridges are generally smooth does not confirm a swash origin either. Whether or not an intertidal surface is left smooth or rippled by falling tide levels is more a reflection of the ability of the swash to flatten the ripples formed by wave processes, than an indication of the dominant hydrodynamic process. Finally, observations on most ridge and runnel beaches reported in the literature suggest that the locations of the ridges are not related to the positions on the intertidal profile where the water level is stationary for the longest time, but are distributed across the entire intertidal profile (Wright, 1976; Orford, 1985; Mulrennan, 1992; Masselink and Anthony, 2001). There is even some evidence to suggest that the largest intertidal ridges are most likely to be found around the mid-tide level, where the swash zone is never stationary (Masselink and Anthony, 2001).

Most ridge and runnel beaches are subjected to semi-diurnal, macrotidal tidal regimes. In such environments, non-stationary water levels due to the tides is an important characteristic of the hydrodynamics. Concurrent with the vertical variation in the water level is the migration of different

hydrodynamic zones across the beach profile (Masselink, 1993). Almost all ridges are expected to experience at some stage during the neap-to-spring tidal cycle a mixture of swash, surf zone and shoaling wave processes (and aeolian processes during periods of emergence). The frequency of occurrence of each of these processes, not to be mistaken for their relative importance, will vary spatially across the intertidal profile and temporally with changing wave/tide conditions.

It seems imperative that any study aimed at investigating the formation and maintenance of ridge and runnel morphology must address the spatial and temporal variation in the relative importance of the different hydrodynamic processes. However, despite an resurgence of interest in ridge and runnel morphodynamics (Voulgaris et al., 1996, 1998; Levoy et al., 1998; Sipka and Anthony, 1999; Chauhan, 2000) none of these recent studies have addressed this. Masselink and Anthony (2001) suggested that it is possible, if not probable, that swash and surf zone processes work in concert to develop and maintain ridge and runnel morphology. They further suggested that to investigate this hypothesis, comprehensive field measurements complemented by numerical modelling are required.

The objective of this paper is to investigate the relative importance of swash and surf zone processes in maintaining ridge and runnel morphology. Detailed morphological and hydrodynamic measurements were conducted on a ridge and runnel beach over a 2-week period. The field observations are subsequently used in conjunction with a numerical model to determine to what extent the observed morphological changes can be attributed to swash and surf zone processes.

2. Study area

The field experiment was conducted on Theddlethorpe beach, North Lincolnshire coast, England (Fig. 1). The beach is located at the southern end of a 20-km long coastal section which is part of the ebb tidal delta of the Humber estuary. The area is characterised by long-term accretion (King, 1972; Halcrow, 1988) and is devoid of coastal engineering structures. The beach morphology is characterised by numerous well-developed intertidal bar systems ('ridge and runnel' morphology) intersected by tidal drainage channels (Masselink and Anthony, 2001). The intertidal bars front an up to 2.5 km wide salt marsh and/or a sand flat. The salt marsh/sand flat area is located just below Mean High Water Spring (MHWS) level and its width progressively decreases toward the south. On Theddlethorpe beach, the sand flat is 400 m wide, but 2 km south of the beach, the intertidal bars are directly backed by sand dunes.

The mean spring tide range in the region is 6 m and the tide levels are: Mean Low Water Spring (MLWS) = −2.85 m, Mean Low Water Neap (MLWN) = −1.25 m, Mean High Water Neap (MHWN) = 1.55 m and MHWS = 3.15 m (all in m ODN, where ODN refers to Ordnance Datum Newlyn, which is approximately mean sea level (MSL)) (Admiralty Tide Tables, 2000; principal port Immingham and secondary port Skegness). Tidal currents generally flow in a southward direction during the flood following the coastal outline and in a northward direction during the ebb (Admiralty Tidal Stream Atlas, 1962). Winds are predominantly from the southwest, however, during the winter months the development of high pressure systems over northern Europe can lead to prolonged northwesterly to easterly winds (Odd et al., 1995). Annual wave statistics have been compiled by the Department of Energy (1989) and indicate a 50% and 10% exceedence significant wave height for the Lincolnshire coast of 0.5 m and 1.5 m, respectively, and a most common wave period of less than 4 s. The sediment transport along the Lincolnshire coast is primarily wave-driven and wave energy calculations suggest that beach sediments are transported southwards from Donna Nook (Halcrow, 1988).

3. Methods

3.1. Field methods

Fieldwork was conducted in July and August 2000. Aerial photographs of the beach were taken

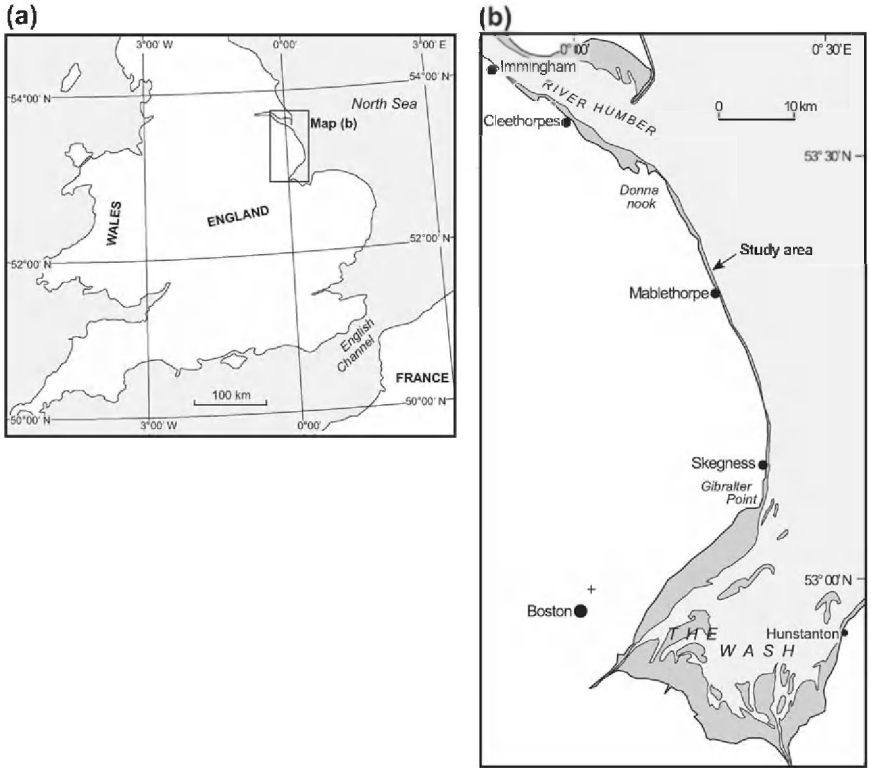

Fig. 1. Location map of the study area. The dark grey areas in (b) indicate intertidal regions.

on 5 August by the Environment Agency and give a good indication of the beach morphology at the time of the field experiment (Fig. 2). The experimental design was very much dictated by the morphology present. A cross-shore transect was established at the start of the field period, starting in the dunes and extending almost 1 km seaward across the intertidal sand flat and beach. Temporary benchmarks were established in the dunes and these were tied to a permanent benchmark with known elevation (in m ODN). The main transect was surveyed every daylight low tide from 31 July to 16 August using a laser total station. During these surveys, detailed observations on the bed morphology were made as well. Information on the 3-D configuration of the intertidal beach was obtained on 3 and 4 August by surveying an extra eight transects 50, 100, 150 and 200 m at either side of the main transect. These measurements were used to generate a digital elevation model (DEM) of the intertidal zone. A large number of sediment samples (about 200) were collected from the upper intertidal sand flat area and the region with the intertidal bar morphology during the 3-D survey. These samples were analysed in the laboratory using a settling tube and the fall velocities obtained from the analysis were converted to sediment sizes using formulae predicted by Gibbs et al. (1971).

During three tidal cycles (5, 7 and 9 August), high-resolution (temporal and spatial) morphological measurements were conducted. On each of these days, a cross-shore transect across the intertidal bar morphology was established about 50 m north of the main transect using 0.8-m long, fibreglass rods inserted into the beach at regular intervals (spacing 1 or 2 m). The locations of the rods and the elevations of their tops were measured at low tide using the total station. As the rods became inundated by the rising tide, their heights above the sand surface were monitored using a specially designed ruler. Only a few rods

had to be measured at the start of the measurements because most of the rods were emerged. This only required a few minutes. However, as the tide rose, the number of rods that were affected by wave and swash processes progressively increased and the time required conducting the measurements increased accordingly. Measurements were conducted approximately every 15 min. Rods that were covered by more than 0.75 m of water could not be reliably measured. These rods were 'abandoned' during the rising tide, but 'revisited' as the tide fell. The above method of obtaining detailed information on morphological change has also been used by Masselink et al. (1997). The vertical accuracy of the measurements is considered better than 1 cm. Concurrent with the rod measurements, observations were made of the bed morphology (plane bed, washed-out ripples, wave ripples) and the hydrodynamic process that the rods were experiencing (swash action, surf zone bores, breaking waves, shoaling waves).

Hydrodynamic measurements were made using three, self-logging instrument frames. These frames were positioned on the intertidal beach. Frame 1 was positioned most seaward at the bottom of the seaward slope of the fourth intertidal bar and consisted of a pressure sensor and a 3-D acoustic current meter (ACM). The ACM was installed such that it measured currents 0.15 m above the bed. The frame was deployed from 1 to 14 August and the data were collected in burst-mode with an interval of 30 min. The burst was 512 data points collected at 2 Hz yielding data sections of 4 min and 16 s. There were two problems with the data. First, because the frame was deployed in the intertidal zone, no data were collected under low tide conditions, except during neap low tide. Second, due to problems with the equipment software, two gaps were present in the data record. In order to obtain a continuous water-level record for the field experiment, tide gauge data collected at Immingham (located 35 km north of the study area) and Boy Grift (15 km south of the study area) were used to complement the water-level data collected by Frame 1. Cross-correlations were conducted between the three data sources and these were subsequently used to interpolate the missing data sections in the water-level record measured on Theddlethorpe beach. Frame 2 was generally positioned on the seaward slope of the third bar and Frame 3 was usually deployed on the seaward slope of the second bar. Frames 2 and 3 each comprised of a pressure sensor, a 2-D, electromagnetic current meter (EM) and an optical back scatterrance sensor (OBS). The EM and OBS on each of the frames were installed to take measurements at 0.15 m above the bed. The frames were deployed from 3 to 15 August and the data were collected in burst-mode with an interval of 1 h. The burst was 4800 data points collected at 2 Hz yielding data sections of 40 min.

The local wave height H_s, wave period T_s and water levels h at Frames 2 and 3 were computed over series of 10 min with a traditional wave-by-wave statistics approach. In addition, the asymmetry of the wave form was computed using two methods. The wave skewness A (or horizontal asymmetry) was defined as the height of the wave crest divided by the total wave height. A saw-tooth parameter B (or vertical asymmetry) was defined by the time span of the wave front passage divided by the total wave period. The values for these wave asymmetry parameters are 0.5 under symmetrical waves and increase with increasing asymmetry.

3.2. Numerical methods

The time that certain processes like shoaling waves, breaking waves, surf zone bores and swash action were operating on a specific position along the central cross-shore profile was computed with a simple model based on water levels. The water levels on the intertidal beach were supposed to be composed of the tidal water level, the wave set-up level and the wave run-up level. The tidal water levels were directly measured offshore. The water levels related to the waves were computed with the use of constant wave conditions or the local wave characteristics measured at Frame 2. The combined effect of wave set-up and wave run-up were computed with (Holman, 1986, in Komar, 1998):

$$R = 0.36 g^{0.5} H_o^{0.5} T \tan\beta \quad (1)$$

where R is the wave run-up height exceeded by 2% of the run-up events (surrogate for the maximum run-up height), g is acceleration of gravity, H_o is the deep-water wave height, T is the wave period and $\tan\beta$ is the beach gradient.

The model computes the local water levels at distinct positions over the cross-shore profile by adding the measured tidal levels and the computed wave-related levels. An attenuation coefficient (i.e. irregular wave breaker criterion) of 0.35 was used to compute the breaker depth out of the local wave height. The processes at a certain location were subsequently coupled to specific local conditions. Shoaling waves occurred when the local water depth exceeded the breaker depth. Breaking waves and surf zone bores occurred when the local water depth was smaller than the breaker depth and when the position was constantly under water. Swash action occurred when the local water level was between the tidal water level and the wave run-up level on the beach. The spatial distribution of shoaling waves, surf (breaking waves and bores) and swash were computed for every minute during a semi-diurnal flood period. This resulted in spatial patterns of process characteristics over the cross-shore profile, as well as their relative contribution over a tidal cycle.

4. Results

4.1. Beach morphology and sedimentology

The intertidal morphology of Theddlethorpe beach is shown in Figs. 2 and 3. The salient features of the beach profile are: (1) a 400-m wide, sub-horizontal ($\tan\beta = 0.0015$) intertidal sand flat located just below MHWS level; and (2) a 400-m wide, gently sloping ($\tan\beta = 0.015$) region with pronounced intertidal bar morphology. At the time of the field experiment, six intertidal bar systems were present, and a seventh subtidal bar system was also observed (but not surveyed). The cross-shore profile shows all six intertidal bars (Fig. 3a), which are numbered 1–6 in the seaward direction. The largest bar, both in terms of width and height, can be found around MSL (bar 4), whereas the seawardmost bar (bar 6) is least pronounced.

Figs. 2 and 3 indicate that the bar morphology is relatively continuous in the longshore direction. However, a relatively large drainage channel south of the main transect intersects bars 3 and 4 and two smaller drainage channels can be observed cutting through bar 1. Bar 1 peters out in a northward direction, while bar 2 merges with bar 3 south of the main transect. The DEM (Fig. 3b)

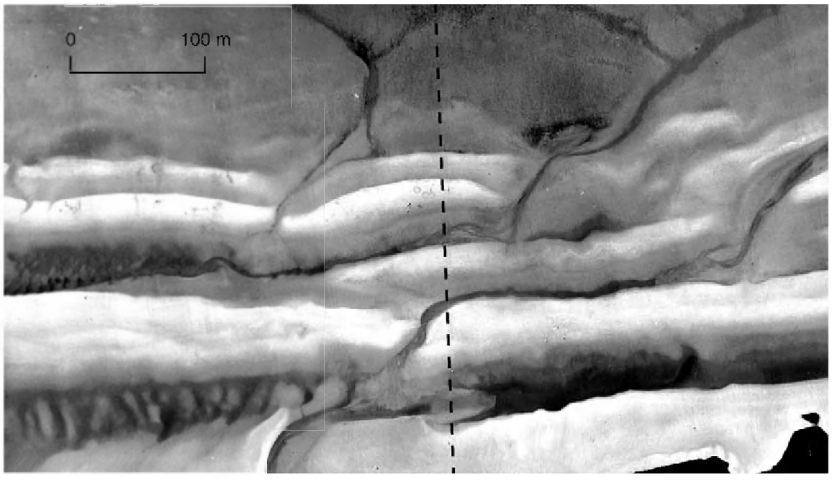

Fig. 2. Aerial photograph of the study area taken on 5 August. The location of the central transect is indicated by the dashed line. Dark sections in the photograph represent small drainage channels and runnels, whereas the ridges are indicated by the light areas.

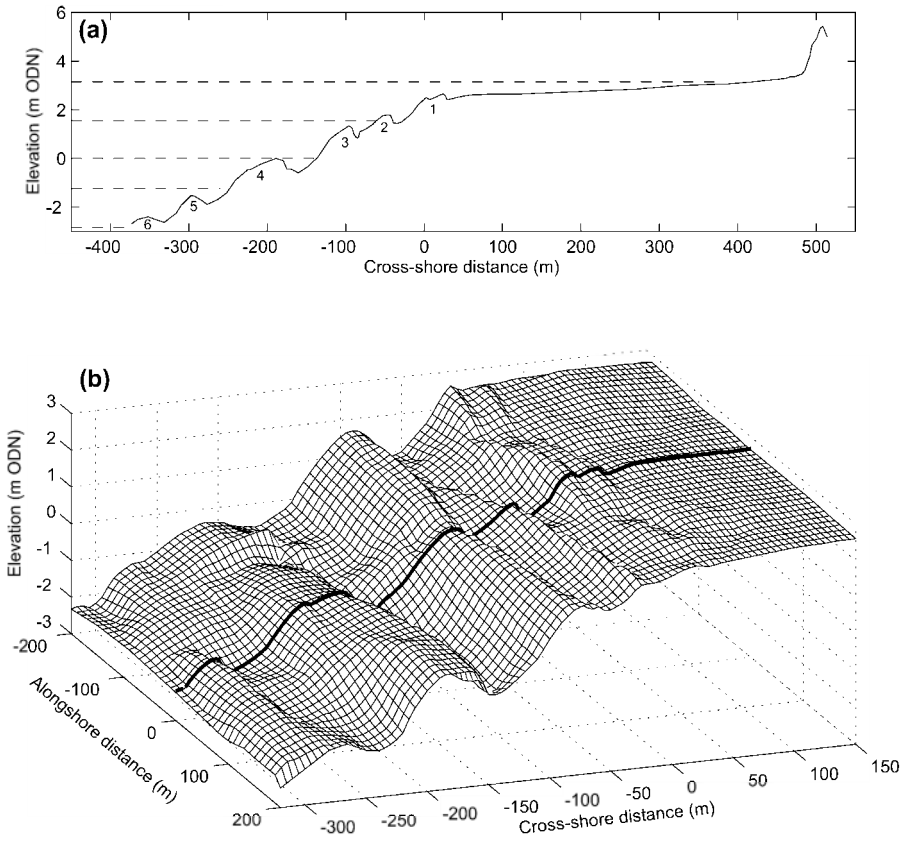

Fig. 3. (a) Beach profile measured on 4 August. Horizontal lines indicate, from top to bottom, MHWS, MHWN, MSL, MLWN and MLWS. (b) 3-D beach profile measured on 3 and 4 August. Thick solid line indicates the central transect. The alongshore coordinates (y-axis) run from south (negative values) to north (positive values).

clearly shows that bar 1 actually consists of two bar crests. The appearance of bar 1 in the field was that of two depositional lobes (see also Fig. 2).

Analysis of the intertidal sediments revealed a distinct textural break around MSL. The D_{50} values of all sediments collected above MSL are within the range 0.18–0.21 mm, whereas the range of D_{50} values for the samples taken below MSL is 0.16–0.18 mm. No significant difference in sediment size was found between intertidal bars, intertidal troughs and upper intertidal sand flat. It should be noted, however, that veneers of mud were generally present in the deeper parts of the intertidal troughs and also on the surface of the lower intertidal bars. Such mud veneers did not occur on the higher intertidal bars.

The intertidal bar morphology can be subdivided into four distinct morphodynamic sub-environments on the basis of morphology, sedimentology and hydrodynamic processes.

(1) The trough is dominated by tidal currents and shoaling/reforming waves. Current ripples are present in the deepest part of the trough, but wave-current and wave ripples may be found at higher levels.

(2) The seaward slope of the bar is affected by a mixture of swash, surf zone and shoaling wave processes. The slope has a convex shape with the local gradient decreasing in the landward direction. Plane beds generally prevail if the local gradient is >0.025 (lower part of the slope), whereas washed-out wave ripples occur when the local gradient is <0.025 (upper part of the slope).

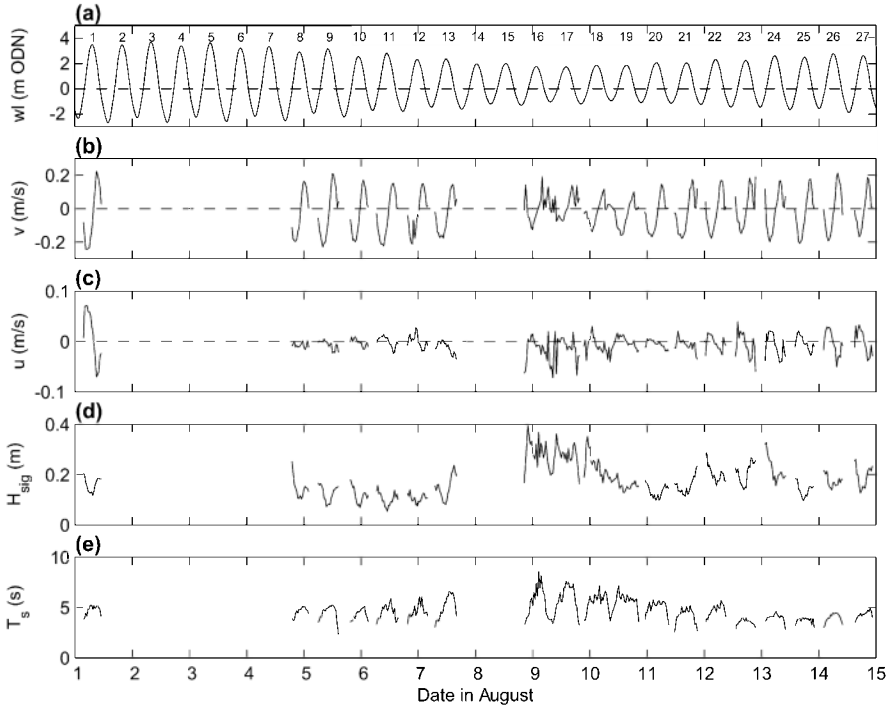

Fig. 4. Tide and wave conditions during the field experiment in 2000. (a) Water level. (b) Longshore current velocity. (c) Cross-shore current velocity. (d) Significant wave height. (e) Significant wave period. Positive longshore and cross-shore currents are toward the north and onshore, respectively. The tidal cycles that occurred over the field period are numbered 1–27 in (a) for later reference.

A narrow zone (several m's wide) of washed-out wave ripples is usually found at the base of the seaward slope. This zone occurs at the same elevation as the crest of the bar located to the seaward and marks the transition from trough to bar.

(3) The landward slope of the bar extends from the bar crest to the brink point (top of the slip face) and is generally sub-horizontal. The region is occasionally subjected to unidirectional pulses of water running into the trough when waves overtop the bar crest. More frequently, the landward slope of the bar will experience surf zone and shoaling wave action. Commonly, the bed is characterised by washed-out wave ripples, rhomboid ripples and/or wave-current ripples.

(4) A slip face is present on all intertidal bars, except for bar 6. The most common sedimentological features on the surface of the slip face were waterline marks and drainage rills.

4.2. Hydrodynamics during the field experiments

The tidal water level, nearshore currents and waves during the 2-week field experiment are shown in Fig. 4. Time-averaged longshore and cross-shore currents indicate a strong tidal modulation (Fig. 4b,c). Southward and onshore currents prevail during the rising tide, whereas northward and offshore currents occur during the falling tide. The mean longshore current attains a maximum velocity of 0.25 m/s during spring tides and is about 0.15 m/s during neap tides. The residual longshore current is negligible. The mean cross-shore current is generally on the order of a few cm/s and only exceeds 0.05 m/s during the largest spring tides. Significant wave heights varied from 0.1 to 0.4 m and significant wave periods were 4–7 s. The waves generally approached the beach with their crests parallel to the coast. It is noted that the most energetic

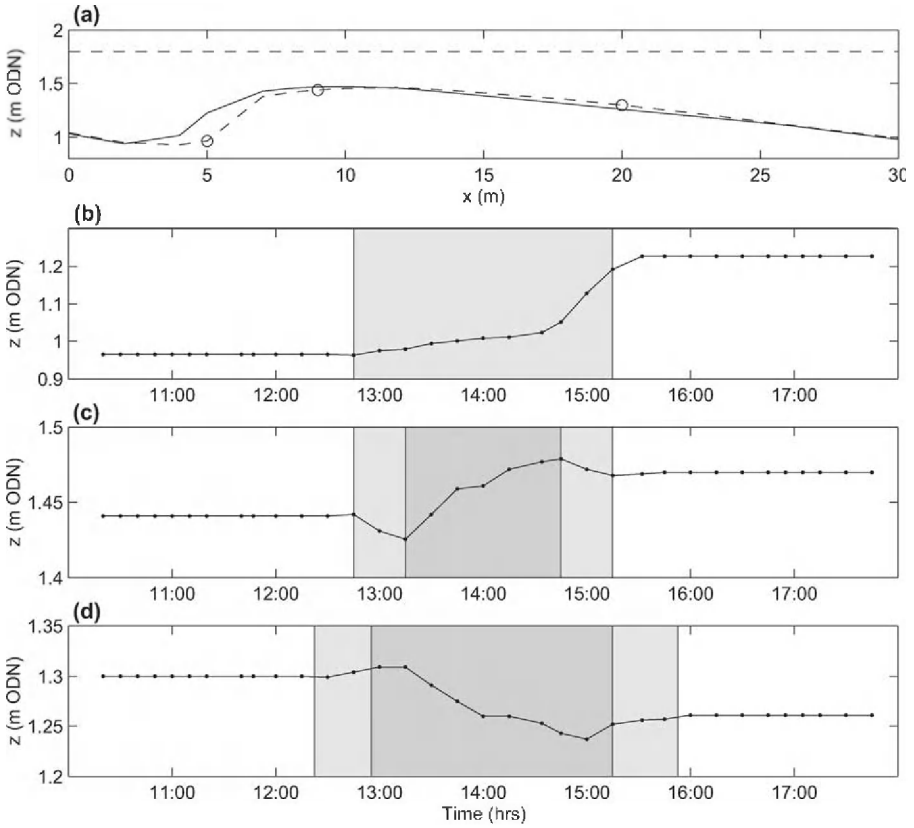

Fig. 5. (a) Beach profiles of bar 3 measured on the morning (dashed line) and evening (solid line) on 9 August. Horizontal dashed line indicates the high tide water level. Open circles indicate locations for which bed level changes are shown in figures below. (b) Changes in bed elevation measured during tidal cycle at $x = 5$ m. Shading indicates the time when wave and swash action took place on the bar crest. (c) Changes in bed elevation measured during tidal cycle at $x = 9$ m. Light and heavy shading indicates the time when swash and surf zone bores were operating at $x = 9$ m, respectively. (d) Changes in bed elevation measured during tidal cycle at $x = 20$ m. Light and heavy shading indicates the time when swash and surf zone bores were operating at $x = 20$ m, respectively.

wave conditions coincided with neap tidal conditions.

4.3. Morphological change over a tidal cycle

Continuous morphological monitoring of a 2–3 intertidal bar system was conducted during three tidal cycles on 5, 7 and 9 August. The data collected on bar 3 on 9 August (tide number 17; Fig. 4a) are summarised in Fig. 5 (data collected during 5 and 7 August were similar, but less prominent due to reduced wave conditions, Fig. 4d). During the tidal cycle, the intertidal bar migrated onshore through deposition on the slip face and the landward slope of the bar, and erosion on the seaward slope (Fig. 5a). The results can best be discussed within the context of the three morphological regions comprising the intertidal bar system: (1) the slip face of the bar ($x = 4$–7 m); (2) the landward slope of the bar from the brink point to the crest of the bar ($x = 7$–12 m); and (3) the seaward slope of the bar ($x = 12$–30 m).

Onshore migration of the bar and sediment accretion on the slip face occurred continuously around high tide while the bar crest was covered by waves and swash (Fig. 5b). Accretion commenced as soon as the incident waves started overtopping the bar crest during the rising tide and accretion ceased when the bar crest became exposed during the falling tide. Most of the sedi-

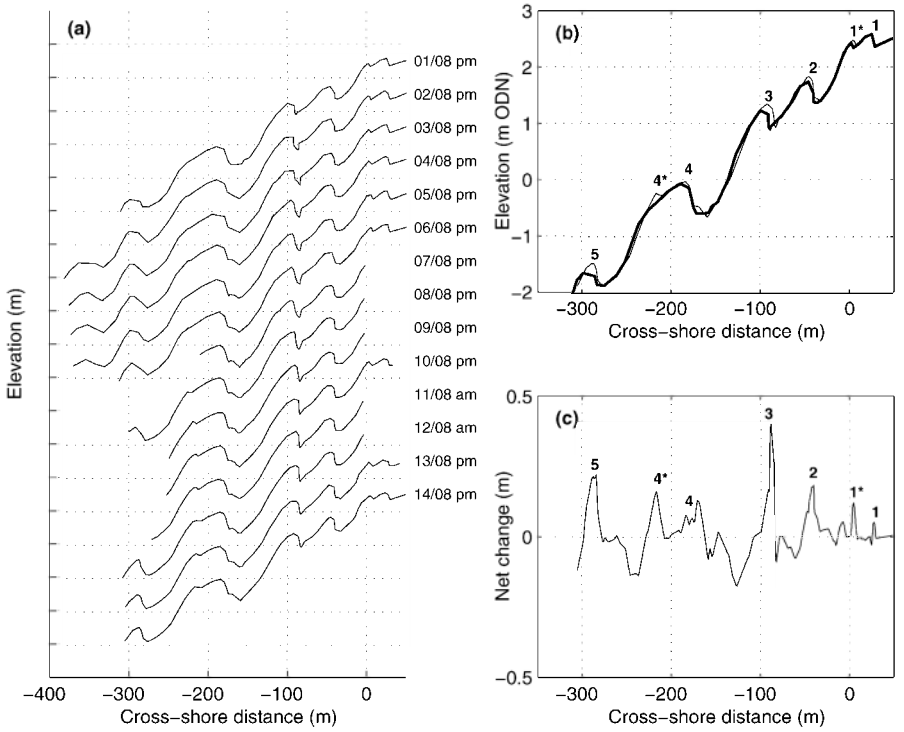

Fig. 6. (a) Daily beach profiles of the central transect. The profiles have been vertically offset by 1 m. The spacing of the vertical ticks marks is also 1 m. (b) Beach profile measured on 1 August (thick solid line) and 14 August (solid line). The intertidal bars are numbered 1–5 in the offshore direction. (c) Morphological change between 1 and 14 August. Positive values indicate accretion, negative values indicate erosion.

ment deposited on the slip face was delivered by swash and waves operating on the intertidal bar, but part of the sediment was washed from the side of the trough by waves refracting around the flanks of the intertidal bar. The landward slope was subjected to a mixture of swash and surf zone bores. At high tide, the water depth over the bar crest was about 0.3 m. When the region was under the influence of swash action, both during rising and falling tides, the flow mainly consisted of wave uprush. The water would rush across the region and shunt sediment into the runnel, resulting in slip face accretion and bar migration (Fig. 5c). Limited erosion of the landward slope occurred under these conditions. When the landward slope was under the influence of surf zone bores, however, accretion prevailed. The net change over the tidal cycle on the landward slope was 3–5 cm accretion. The seaward slope of the bar was also subjected to a mixture of swash and surf zone processes. However, in this region, swash processes resulted in sediment accretion, whereas surf zone bores caused erosion (Fig. 5d). The net change on the seaward slope was 2–4 cm erosion.

Most significantly, Fig. 5 demonstrates that morphological change on the intertidal, in particular the erosion of the seaward slope, occurs primarily under the influence of surf zone bores. Swash action has a significant effect on the morphology, but is secondary to that of surf zone bores. The location of the swash and bores also heavily depends on the antecedent morphology.

4.4. Morphological change over spring-to-spring tidal cycle

In a general sense, the amount of morphological change over the 2-week period of observations was quite limited. The number of intertidal

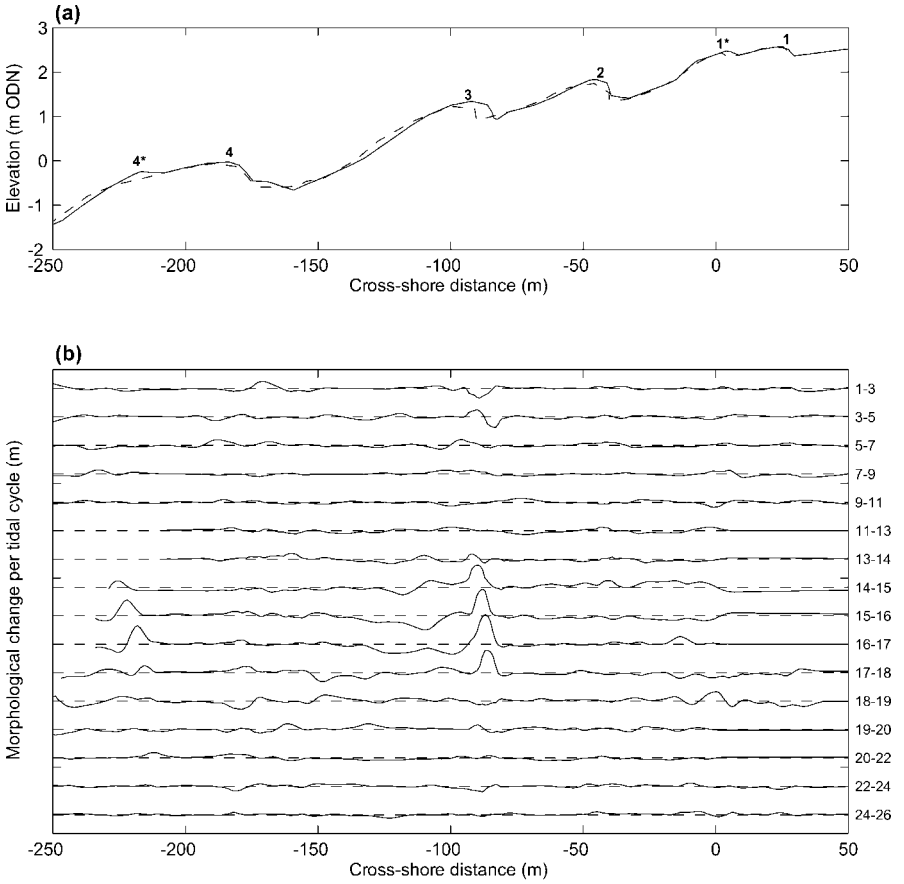

Fig. 7. (a) Beach profile measured on 1 August (dashed line) and 14 August (solid line). (b) Morphological change per tidal cycle derived from daily or twice-daily beach profiles. The morphological change profiles have been vertically offset by 0.15 m. Positive values indicate accretion, negative values indicate erosion. The numbers on the right-hand side of (b) refer to the tide numbers in Fig. 4a. For example, the label 9–11 indicates the change in morphology derived from beach profiles measured after tide 9 and 11. About half the morphological change profiles represent changes that occurred over two tidal cycles. For these, the observed morphological change has been halved to represent the morphological change per tidal cycle.

bars remained the same and none of the bars were modified to any great extent (Fig. 6a). However, comparison of the first (1 August) and last profile (14 August) reveals several interesting features (Fig. 6b,c). All intertidal bars experienced landward migration, in particularly bar 3, which migrated 7–8 m. Onshore bar migration was accomplished by the transfer of sediment from the seaward slope of the bar (erosion) to the landward slope and slip face (accretion). Over the 2-week period, the sediment budget in the intertidal zone was slightly positive, with a net influx of sediment of 4.2 m^3 per unit metre width. This equates to a net sediment transport from the subtidal to the intertidal zone of 0.15 m^3 per unit metre width per tidal cycle. This is a very small amount of sediment and it can be concluded that mass has practically been conserved over the measurement period. A lobe formed on the seaward slope of bar 4 during the second half of the monitoring period (after 9 August), making the bar 'double-crested' like bar 1.

The daily to twice-daily intertidal profile data were used to determine the morphological change between consecutive surveys ('morphological change profiles'). The morphological change between profiles was generally very small, on the order of cm's, and only slightly less than the ver-

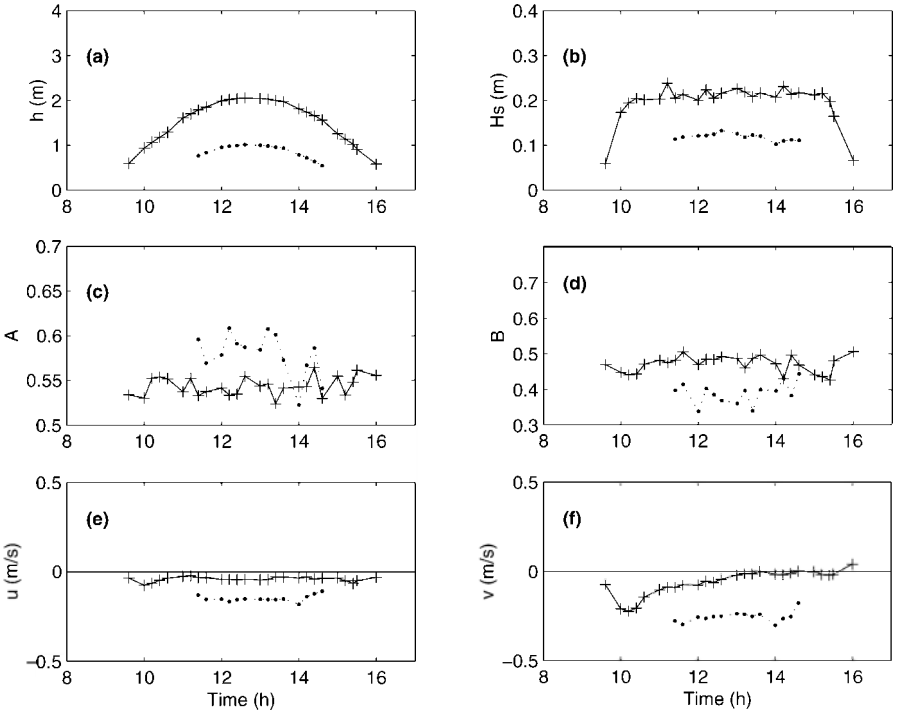

Fig. 8. Variations of the water motion on the seaward slope of bar 2 (dots) and bar 3 (crosses) over tide number 15. (a) Local water depth h. (b) Significant wave height H_s. (c) Wave skewness A. (d) Saw-tooth parameter B. (e) Mean cross-shore velocity u. (f) Mean alongshore velocity v.

tical accuracy of the measurements. To reduce the effect of (random) measurement error on the results, the cross-shore variation in morphological change was smoothed with a 5-m wide moving average. Finally, the morphological change profile was detrended to remove inaccuracies in the vertical datum between the profiles.

The morphological change profiles are shown in Fig. 7. Onshore migration of bars 1–3 occurred at the start of the field period (1–5 August; tide number 1–9) when large spring tidal ranges of up to 6 m were experienced (Fig. 4a). In addition, the trough to the landward of bar 3 was deepened significantly, whereas the trough landward of bar 4 underwent accretion through the progradation of a drainage delta present just to the south of the central survey line (Fig. 2). The high tide level during these spring tides exceeded 3 m and resulted in the submergence of the intertidal bar morphology and inundation of the upper intertidal flat. During neap tide conditions and elevated wave energy levels in the middle of the field period (7–10 August; tide number 13–18), onshore migration of bars 2–4 occurred. Bar 3 exhibited the most dynamic behaviour and experienced landward migration rates of about 1 m per tide. In addition to the onshore migration of the intertidal bars, a small lobe was deposited on the seaward slope of bar 4. The sediment required to form this depositional feature was eroded from lower on the profile, resulting in a steepening of the local profile. Toward the end of the field period (10–14 August; tide number 19–27), the tidal range increased and wave energy levels were low. Not many morphological changes occurred. Of note is the formation of a small lobe on the seaward slope of bar 1 at the end of the field period (tide number 22–26).

4.5. Swash and surf zone processes on intertidal bars

The swash and surf zone processes were strongly coupled to the local water depth. The

Table 1
Measured significant wave heights, wave periods and tidal ranges for the numerical simulations of the cross-shore intertidal process characteristics

Date	Tide (number)	H_s (m)	T_s (s)	Tidal range (m)
1-08-2000	1	0.20[a]	6.0[a]	5.84
	2	0.20[a]	6.0[a]	5.75
2-08-2000	3	0.20[a]	6.0[a]	6.36
	4	0.20[a]	6.0[a]	6.09
3-08-2000	5	0.20[a]	6.0[a]	6.23
	6	0.20[a]	6.0[a]	5.82
4-08-2000	7	0.20[a]	6.0[a]	5.88
	8	0.13	4.8	5.45
5-08-2000	9	0.09	4.2	5.36
	10	0.13	4.0	4.79
6-08-2000	11	0.10	4.2	4.60
	12	0.09	4.8	4.11
7-08-2000	13	0.09	5.6	3.99
8-08-2000	14	0.17	5.7	3.59
	15	0.22	6.3	3.32
9-08-2000	16	0.29	6.1	3.07
	17	0.27	6.6	2.91
10-08-2000	18	0.22	5.7	3.04
	19	0.16	5.6	2.97
11-08-2000	20	0.12	5.2	3.21
	21	0.14	4.7	3.30
12-08-2000	22	0.18	5.2	3.78
	23	0.17	3.7	3.70
13-08-2000	24	0.20	4.2	4.27
	25	0.13	3.9	4.16
14-08-2000	26	0.20[a]	6.0[a]	4.68
	27	0.20[a]	6.0[a]	4.53
15-08-2000	28	0.20[a]	6.0[a]	5.05

[a] Standard wave conditions (not measured)

local water motions on the seaward slope of bars 2 and 3 were measured with the stand-alone frames. An example of the characteristics of the water motion over tide number 15 is presented in Fig. 8. The local water depth h showed the tidal curve (Fig. 8a) and the significant wave height H_s was almost constant in time and reached a value of 0.12 m on the slope of bar 2 and 0.22 m on the slope of bar 3 (Fig. 8b). The larger wave heights on bar 3 occurred because at high tide waves were breaking on both bars crests and incident waves were significantly attenuated when propagating across bar 3. The shape of the waves on bars 2 and 3 was distinctly asymmetric. The wave skewness A reached a value of 0.6 at the slope of bar 2 and a value of 0.55 at the slope of bar 3 (Fig. 8c). The saw-tooth parameter B ranged between 0.3 and 0.4 at the slope of bar 2 and ranged between 0.4 and 0.5 at the slope of bar 3 (Fig. 8d). The mean cross-shore velocity u was small and offshore directed. At the slope of bar 2, a maximum offshore-directed value of 0.15 m/s occurred. The u at the slope of bar 3 was constant at about 0.05 m/s (Fig. 8e). The mean alongshore velocity v reached maximum values of about 0.25 m/s and showed northward flowing currents during rising tide (Fig. 8f).

The values for the wave asymmetry parameters A and B at the seaward slope of bar 2 were far off the standard value of 0.5, typical of symmetrical waves. This implied that the waves at this location were propagating as bores. Values for A and B at the seaward slope of bar 3 also indicated that asymmetric waves were present, but especially the value of B was close to 0.5. This implied that the waves at this location were propagating as asymmetric shoaling waves. Unfortunately, all measurements required a water depth over 0.3 m in order to get reliable data over 10 min. All measured cross-shore velocities at 0.2 m above the bed were still offshore-directed. Onshore-directed flows were observed in the field at the crest of the bars when the water depth was less than 0.2 m.

4.6. Numerical simulations of the local process characteristics

The numerical model described in Section 3.2 was used to compute the temporal and spatial variation in the occurrence of swash, surf zone and shoaling wave processes across the intertidal beach profile. The measured tidal water levels and wave conditions were used as input variables for the numerical simulations of the local process characteristics over a measured intertidal barred profile (Table 1). Additionally, the measured tidal water levels and two constant wave conditions ($H_s = 0.1$ m, $T_s = 4$ s; $H_s = 0.2$ m, $T_s = 6$ s) were used to study the variability of the process characteristics over the whole spring-to-spring tidal cycle of the field experiments.

The modelled cross-shore distribution of swash and surf (breaking waves and bores) over the barred intertidal profile during a spring flood is

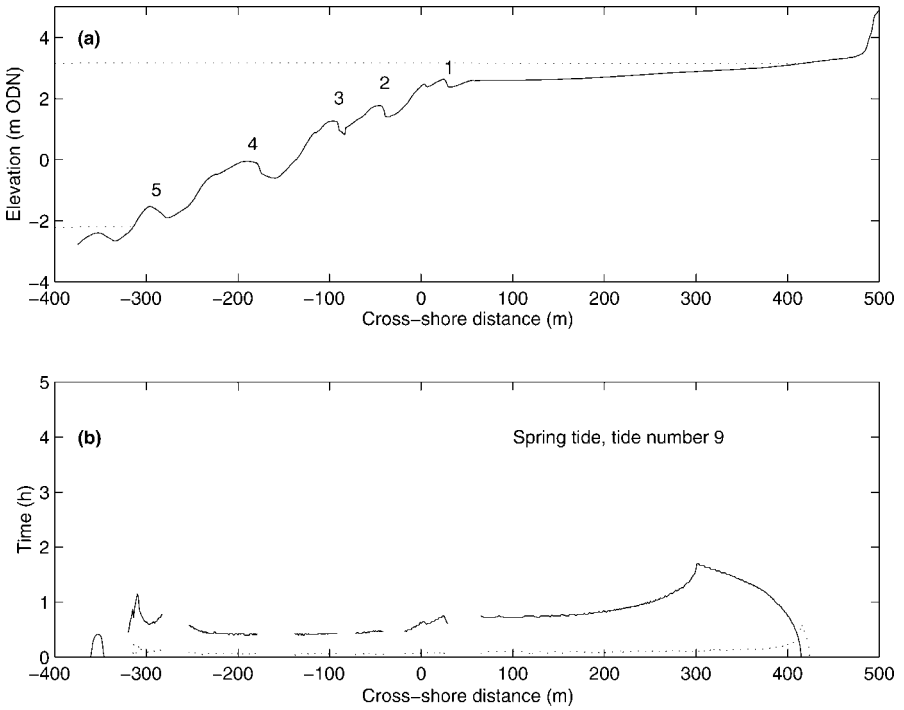

Fig. 9. (a) Beach profile along the central transect with the projected high and low water levels during a spring tide. (b) Numerical simulations of the cross-shore distribution of surf (breaking waves and bores; line), and swash (dotted line) during a spring flood.

presented in Fig. 9 (tide number 9; tide range 5.4 m; $H_s = 0.1$ m). Due to the large tidal range, and hence tidal translation rates, swash and surf zone processes rapidly shift over the profile and all intertidal bars experience approximately the same time of each of these processes. The swash is only active for a couple of minutes at each bar location and the surf zone processes operate for 30 min to 1 h in the barred area. These periods are too short to cause significant modifications in the morphology of any of the intertidal bars (morphological changes were less than 1 cm; Fig. 7b).

Simulation results for a neap flood are presented in Fig. 10 (tide number 17; tide range 3.0 m; $H_s = 0.3$ m). Swash and surf zone processes are spread between bars 2 and 5. The peaks in the spatial distribution of both process characteristics are at the locations of the intertidal bars. At bar 2, the swash action is most prominent and plays a role over more than 1 h, followed by the surf. At the other bar crests (bars 3–5), surf zone processes operate for more than 2 h at one location, with a maximum of about 4 h near bar crest 3. The swash on bars 3–5 is also more prominent than in the spring tide case and reaches time spans of about 30 min. The periods that the swash and the surf act on the profile are sufficient to cause morphological changes near some of the bars. In addition, it should be pointed out that the waves in the neap tide case were significantly more energetic than in the spring tide case. The combined action of swash and surf were responsible for the onshore migration of bar 3 and the formation of a small depositional lobe on the seaward slope of bar 4 (Fig. 7b).

The duration of swash and surf zone processes at bar crests 1–5 over the spring-to-spring tidal cycle are presented in Fig. 11. These durations have been computed using measured tidal levels and measured wave conditions for tide numbers 8–25 (see Table 1) and standard wave conditions

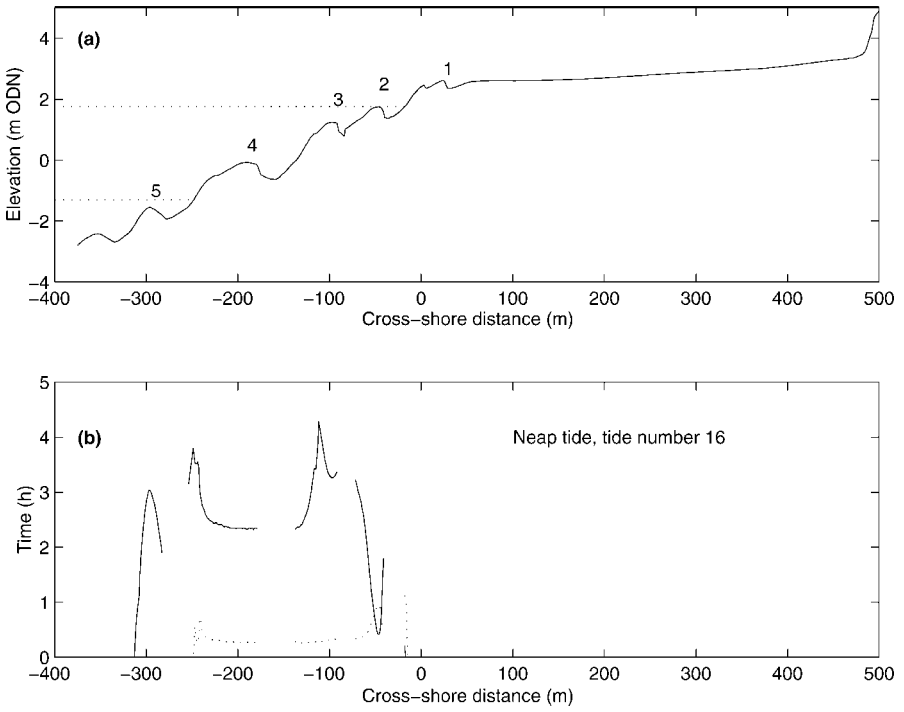

Fig. 10. (a) Beach profile along the central transect with the projected high and low water levels during a neap tide. (b) Numerical simulations of the cross-shore distribution of surf (breaking waves and bores; line), and swash (dotted line) during a neap flood.

of $H_s = 0.2$ m and $T_s = 6.0$ s for tide numbers 1–7 and 26–28. Bar 1 was intertidal during the spring tides and subaerial during the neap tides. The swash and especially the surf on 4–6 August (tide numbers 8–11) operated at the crest of this bar between 1 and 2 h. The surf zone bores may have caused modest morphological changes at bar 1 as observed in Fig. 7b. Bar crest 2 was halfway across the intertidal area during spring tide and close to the high water line during neap tide. The influence of surf zone bores increased from spring towards neap tide and only decreased at the neap tide itself when the swash was dominant. Most of the time, the bores and the swash did not operate long enough at a certain location to cause significant morphological changes. Only the swash and surf action at 6–9 August (tide numbers 12–17) caused a small onshore migration of the bar (Fig. 7b). Bar crest 3 was always intertidal. The influence of the swash and especially the surf zone bores increased from spring tide to neap tide. At neap tide, the surf operated between 2 and 4 h a tide over the bar crest (7–10 August, tide numbers 13–19). These bores induced a net onshore transport of sediment during this period, causing an onshore migration of the bar and a concurrent erosion of the seaward slope of the bar (Fig. 7b). The same observations of increasing influence of bores and breaking waves at neap tide apply to bar crest 4. Again, this was also reflected in the morphological changes observed in the cross-shore profiles (Fig. 7b) with an onshore migration of the bar crest and erosion of the seaward side of the bar over the same period. Bar crest 5 was completely submerged during neap tide and intertidal during spring tide. The swash was only of any influence on 8 August (tide number 14). Breaking waves and bores only operated over 2 h two days before and two days after neap tide.

The numerical simulations were also made with constant wave conditions over the whole period

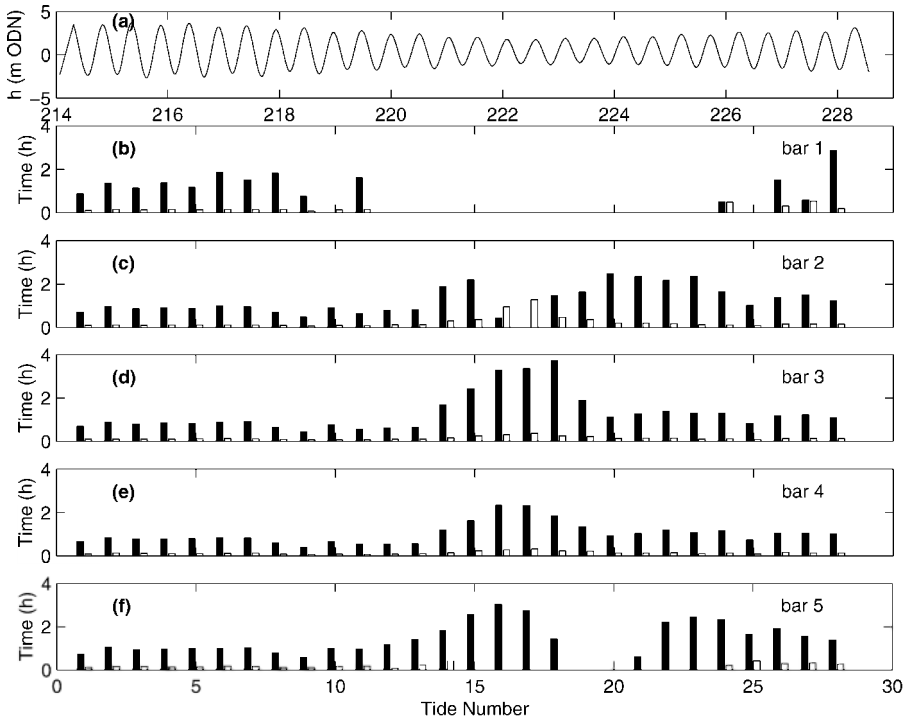

Fig. 11. (a) Measured tidal water levels during the period 1–15 August 2000 (Julian days 214–228). (b–f) Duration of the surf (breaking waves and bores) (black) and swash action (white) during the successive tides at the locations of bar crests 1–5. The simulations are based on a combination of measured and interpolated wave conditions (Table 1).

of the field experiments (1–15 August; tide numbers 1–28). The process characteristics (swash and surf action) at bar crests 1–5 and the measured tidal water levels over the spring-to-spring tidal cycle for waves with $H_s = 0.2$ m and $T_s = 6$ s show very similar patterns as the measured wave conditions presented in Fig. 11. The influence of swash and surf zone processes at spring tide was always less than that at neap tides. At the start of the experiments the swash was no longer than a couple of minutes active over the whole profile and the surf (breaking waves and bores) operated for less than 1 h. Again, the major morphological changes near the bar crests of bar 1–5 could be addressed to the periods that the surf and swash were at least 2 h 30 min working on a certain location. The process characteristics with smaller waves ($H_s = 0.1$ m and $T_s = 4$ s) showed the same spatial patterns but with a smaller intensities (hours).

5. Discussion and conclusions

Intertidal bar morphology was monitored on a macrotidal beach over a spring-to-spring tidal cycle under low-energy, fetch-limited wave conditions ($H_s < 0.3$ m; $T_s = 4$–7 s). The observed morphological changes were very small, but over the 2-week period the intertidal sediment budget was clearly positive and all intertidal bars migrated onshore with rates ranging from insignificant to 1 m per tide. The landward movement of the bars was accomplished by the transfer of sediment from the seaward slope of the bar (erosion) to the landward slope and slip face (accretion). This onshore sediment transport was carried out by a combination of swash and surf zone processes.

The morphological measurements showed that the intertidal bar dynamics exhibited a pronounced spatial and temporal variability. The

most active bar was located around MSL (bar 3) and the largest bar migration rates occurred during neap tide conditions. Bar morphological changes during spring tide conditions were very limited. A simple numerical model was developed to predict the duration of swash/surf processes on the intertidal profile under varying wave/tide conditions. The model results were subsequently used to explain the morphological observations. It was found that the most important factor controlling bar morphological change (i.e. onshore bar migration) is the length of time that the bar crest is under the influence of swash and surf zone processes. During spring tides, the rapid tidal translation rate does not allow these hydrodynamic processes to act sufficiently long (generally less than 30 min) at any location to accomplish significant morphological changes. During or around neap tides, however, swash and surf zone processes may operate for up to 30 min and 2 h, respectively, at the bar locations. It is at these times that the intertidal bars display an onshore migration of the crest and erosion of the seaward side (as shown in Fig. 7b).

The simple numerical model that computes the water level over the cross-shore profiles during the tidal cycle may only be used in case of low-energy wave conditions. Wave transformation is not directly taken into account and the different process characteristics are simply coupled to water levels. During high-energy wave conditions, the model needs to be extended to describe the wave energy decay over the profile more accurate (e.g. Battjes and Janssen, 1978). However, the present model is able to couple the residence time of distinct processes like surf (breaking waves and bores) or swash to morphological changes in a variety of tidal ranges.

The duration of swash and surf action on the intertidal profile does not solely depend on the tide range, but is also affected by the incident wave height. This is because larger wave heights are associated with wider swash and surf zones, thereby increasing the duration of each of these processes for a given tidal range. According to Masselink (1993), the duration of different types of hydrodynamic processes (swash, surf and shoaling waves) on the intertidal beach profile is governed by the ratio of tide range to wave height, referred to as the relative tide range RTR. During the field experiment, the most energetic waves coincided with neap tide conditions (Fig. 4). Therefore, the relative tide range during neap tides ($RTR = 10$–20) was considerably less than during spring tides ($RTR = 30$–50). It is of interest to compare the present RTR values with those that characterise the measurements of Sipka and Anthony (1999) who also measured morphological change and wave/tide conditions on a macrotidal beach with intertidal bar morphology. During their experiment, Sipka and Anthony (1999) experienced similar wave conditions, but slightly larger tidal ranges. The relative tide range exceeded 30, even during neap tides. Sipka and Anthony (1999) reported that morphological changes over the measurement period were insignificant, perhaps suggesting that significant morphological changes to macrotidal bar morphology require wave/tide conditions characterised by $RTR < 30$.

Intertidal bars on macrotidal beaches are generally considered swash bars whose formation, maintenance and onshore migration of which are controlled by swash processes, while energetic surf zone processes acting during storms result in their flattening or even destruction (King, 1972). This paper does not address bar formation or destruction. However, the data presented here clearly demonstrate that onshore bar migration is mainly accomplished by surf zone processes, with swash processes playing a secondary role (Fig. 5). It thus seems inappropriate to refer to these intertidal bars as swash bars. In fact, when the bars are actively migrating onshore, such as bar 3 during neap tide conditions, they are rather similar in morphology and behaviour to inner surf zone bars. Sunamura and Takeda (1984, p. 70) provided the following description of the onshore migration of such bars: 'When a bar is migrating onshore, wave breaking always occurs over the gently seaward-sloping surface of the bar. Waves after breaking form bores that advance over the bar. Such bores transport sediments onshore across the gently sloping surface, primarily in a bed-load manner, and eventually the material is moved to the steep landward edge of the bar

where it is deposited on the slip-face of the bar.' The above description on inner bar migration is directly applicable to the landward movement of intertidal bars. The only difference between the behaviour of microtidal, inner surf zone bars and macrotidal, intertidal bars is that the inner surf zone bars migrate onshore as long as low-energetic wave conditions persist, whereas the landward movement of the intertidal bars is intermittent and controlled by the tidal water levels.

Acknowledgements

The authors would like to thank Selma van Houwelingen and Aafke Tonk for their assistance during the field experiments in July and August 2000.

References

Admiralty Tidal Stream Atlas, 1962. Tidal Stream Atlas, North Sea, Southern Portion, revised edn. Hydrographic Office, Taunton.

Admiralty Tide Tables, 2000. United Kingdom and Ireland (including European Channel Ports). Hydrographic Office, Taunton.

Battjes, J.A., Janssen, J.P.F.M., 1978. Energy loss and set-up due to breaking of random waves. Proceedings 16th International Coastal Engineering Conference, ASCE, pp. 570–587.

Chauhan, P.P.S., 2000. Bedform association on a ridge and runnel foreshore: Implications for the hydrography of a macrotidal estuarine beach. J. Coast. Res. 16, 1011–1021.

Davis, R.A., Fox, W.T., Hayes, M.O., Boothroyd, J.C., 1972. Comparison of ridge and runnel systems in tidal and non-tidal environments. J. Sediment. Petrol. 2, 413–421.

Department of Energy, 1989. Wave Climate Atlas of the British Isles. OTH 89 303. HMSO, London.

Gibbs, R.J., Matthews, M.D., Link, D.A., 1971. The relationship between sphere size and settling velocity. J. Sediment. Petrol. 41, 7–18.

Halcrow, 1988. The Sea Defence Management Study for the Anglian Region. William Halcrow, Swindon.

Hayes, M.O., Boothroyd, J.C., 1969. Storms as modifying agents in the coastal environment. In: Hayes, M.O. (Ed.), Coastal Environments, NE Massachusetts. University of Massachusetts, Amherst, pp. 290–315.

King, C.A.M., 1972. Beaches and Coasts. Edward Arnold, London.

King, C.A.M., Williams, W.W., 1949. The formation and movement of sand bars by wave action. Geogr. J. 113, 70–85.

Komar, P.D., 1998. Beach Processes and Sedimentation, 2nd ed. Prentice Hall, Upper Saddle River, NJ, 544 pp.

Levoy, F., Anthony, E.J., Barusseau, J.P., Howa, H., Tessier, B., 1998. Morphodynamique d'une plage macrotidale à barres. C.R. Acad. Sci. 327, 811–818.

Masselink, G., 1993. Simulating the effects of tides on beach morphodynamics. J. Coast. Res. Spec. Issue 15, 180–197.

Masselink, G., Hegge, B.J., Pattiaratchi, C.B., 1997. Morphodynamics of a natural beach with beach cusp morphology. Earth Surf. Process. Landf. 22, 1139–1155.

Masselink, G., Anthony, E.J., 2001. Location and height of intertidal bars on macrotidal ridge and runnel beaches. Earth Surf. Process. Landf. 26, 759–774.

Mulrennan, M.E., 1992. Ridge and runnel beach morphodynamics: An example from the Central East Coast of Ireland. J. Coast. Res. 8, 906–918.

Odd, N.V., Baugh, J.V., Murphy, D.G., Cooper, A.J., Oakes, A.M., 1995. Development and Application of Norpoll (MK1.1) to Predict the Effect of Load Reductions on Concentrations of Cadmium and Lead, Particulate Pollutants in the North Sea – Phase II Final Report. Report SR383, HR Wallingford Ltd., Wallingford.

Orford, J.D., 1985. Murlough Spit, Dundrum Bay. In: Whalley, B., Smith, B.J., Orford, J.D., Carter, R.W. (Eds.), Field Guide to Northern Ireland. Queens University, Belfast, pp. 68–76.

Orford, J.D., Wright, P., 1978. What's in a name? Descriptive or genetic implications of 'ridge and runnel' topography. Mar. Geol. 28, M1–M8.

Owens, E.H., Frobel, D.H., 1977. Ridge and runnel systems in the Magdalan Islands. Quebec. J. Sediment. Petrol. 47, 191–198.

Sipka, V., Anthony, E.J., 1999. Morphology and hydrodynamics of a macrotidal ridge and runnel beach under low wave conditions. J. Rech. Oceanogr. 24, 24–31.

Sunamura, T., Takeda, I., 1984. Landward migration of inner bars. Mar. Geol. 60, 63–78.

Voulgaris, G., Mason, T., Collins, M.B., 1996. An energetics approach for suspended sand transport on macrotidal ridge and runnel beaches. Proceedings 25th International Coastal Engineering Conference, ASCE, pp. 3948–3961.

Voulgaris, G., Simmonds, D.J., Michel, D., Collins, M.B., Huntley, D.A., 1998. Measuring and modelling sediment transport on a macrotidal ridge and runnel beach: An intercomparison. J. Coast. Res. 14, 315–330.

Wijnberg, K.M., Kroon, A., in press. Barred Beaches. Geomorphology.

Wright, P., 1976. The Morphology, Sedimentary Structures and Processes of the Foreshore at Ainsdale. Unpubl. Ph.D. Thesis, University of Reading.